Title: The Plasmodium alveolin IMC1a is stabilised by its terminal cysteine motifs and facilitates sporozoite morphogenesis and infectivity in a dose-dependent manner

Article Type: Research Paper

Corresponding Author: Dr. Johannes Dessens, PhD

Corresponding Author's Institution: London School of Hygiene and Tropical Medicine

First Author: Fatimah S Al-Khattaf, PhD

Order of Authors: Fatimah S Al-Khattaf, PhD; Annie Z Tremp, PhD; Amira El-Houderi, MSc; Johannes Dessens, PhD

Abstract: Apicomplexan parasites possess a unique cortical cytoskeleton structure composed of intermediate filaments. Its building blocks are provided by a conserved family of proteins named alveolins. The core alveolin structure is made up of tandem repeat sequences, thought to be responsible for the filamentous properties of these proteins. A subset of alveolins also possess conserved motifs composed of three closely spaced cysteine residues situated near the ends of the polypeptides. The roles of these cysteine motifs and their contribution to alveolin function remains poorly understood. The sporozoite-expressed IMC1a is unique within the Plasmodium alveolin family in having conserved cysteine motifs at both termini. Using transgenic Plasmodium berghei parasites, we show in this structure-function analysis that mutagenesis of the amino- or carboxy-terminal cysteine motif causes marked reductions in IMC1a protein levels in the parasite, which are accompanied by partial losses of sporozoite shape and infectivity. Our findings give new insight into alveolin function, identifying a dose-dependent effect of alveolin depletion on sporozoite size and infectivity, and vital roles of the terminal cysteine motifs in maintaining alveolin stability in the parasite.

Opposed Reviewers:

Dear Andy

Please find a revised version of our manuscript entitled: **"The *Plasmodium* alveolin IMC1a is stabilised by its terminal cysteine motifs and facilitates sporozoite morphogenesis and infectivity in a dose-dependent manner"**, as well as a response letter addressing the reviewer's comments.

Best wishes,

Hans Dessens
Corresponding Author

Response to Reviewers

We thank the reviewers for their input and helpful comments. We have addressed their specific points as follows:

Reviewer #1:

p3, l51-54: Like the protein, the function appears evolutionary conserved, as similar phenotyes were observed in ciliates by El-Haddad, H. et al. (2013; Characterization of TtALV2, an essential charged repeat motif protein of the Tetrahymena thermophila membrane skeleton. Eukaryotic Cell 12, 932-940). Worth mentioning, also because in the ciliate it was not a KO, but a downregulation, too (dose-dependent) and hence similar to what the authors describe for the mutants e.g. on p12 middle section.
To reflect the reviewer's point, we have added the sentence: "In *Tetrahymena thermophila*, knockdown of the alveolin TtALV2 was also reported to affect cell morphology in (El-Haddad et al., 2013)), indicating that alveolin functions, like their structures, are evolutionary conserved." (lines 51-53).

p4, l62: The authors draw a connection between the alveolins and intermediate filaments based on the repeat motifs. Such a comparsion was already explicitly drawn by El-Haddad et al. 2013 and and should mentioned accordingly.
We have added the El-Haddad et al (2013) reference to reflect this (line 58).

p4, l68-70: The CC-motifs have not only been implied in S-palmitoylation. Note: "This CC motif is present in both termini of PfALV1 and TgALV1 but only at the N-terminus of PfALV4, TgALV4, and TpALV2 (fig. 1, arrows). We have not identified a CC motif within dinoflagellate or ciliate alveolins, perhaps suggesting that the motif has a role in either the unique motility of apicomplexa or their unusual modes of cytokinesis." It's from Gould et al. 2008 that you cite, so please mention this.
To reflect the reviewer's point, we have added the sentence: "Because these conserved cysteine motifs have not been identified in alveolins from dinoflagellates or ciliates, their function could be related to the unique motility and/or cytokinesis associated with the Apicomplexa (Gould et al., 2008)." (69-71).

p15, l330-331: on the formation of disulfide bonds and the unfavorable conditions. Correct, and which is why it happens in the IMS of mitochondria and the ER only. This could use a citation and Herrmann and Riemer 2014 might be a good choice (2014; Three Approaches to One Problem: Protein Folding in the Periplasm, the Endoplasmic Reticulum, and the Intermembrane Space. Antioxid. Redox Signal. 21, 438-456).
We have now added this citation.

p18, 402-412. How sure can we be that the single C residue of the carboxy terminus plays no role in processing as it does in Toxoplasma (Mann et al. 2002)? A transgenic line was generated that expresses a full-length version of IMC1a with a C-terminal mCherry tag for the analysis. Could that not influence the ability of the protease to reach the cleavage motif? What is known for other Plasmodium spec.?
To address the reviewer's comment we have added the following to the relevant part of the Discussion section: "It cannot be ruled out that the mCherry tag stopped the protease responsible from reaching the C-terminal cleavage site, preventing the IMC1a cleavage in our parasite lines. Arguing against this possibility, however, is the fact that mCherry tagging of IMC1a did not affect its subcellular localisation or cause a detectable phenotype, which indicates that IMC1a function was not affected." (lines 414-418). It is currently not known what the situation is for other Plasmodium species.

The authors show a post-transcriptional effect on the quantity of IMC1a when the CC motifs are manipulated. The authors discuss the phenotypes, etc. but a bit more reasoning on how and at what point the authors think the levels of protein are reduced would be nice. Is less

protein translated? Seems unlikely, right? The folding (C-C bridges) is unlikely as the authors correctly mention, but can there be no alternative to palmitoylation? See also previous point.

To address the reviewer's comments have added the following sentence to the Discussion section: "We did not observe sporozoites with high (WT) levels of fluorescence in our mutant sporozoite populations. Assuming that IMC1a expression was not affected by the cysteine mutations, this suggests that the reductions in IMC1a levels occurred soon after translation and possibly before IMC1a recruitment to the pellicle". (lines 330-333).

Reviewer #2:

Specific comments
The findings in this manuscript are interesting, specifically the fact that only the deletion of the N-terminal cysteines of IMC1a seem to affect salivary gland invasion more than C-terminal ones. Could it be that they play a regulatory role and apart from their suggested role in Palmitoylation? Alternatively are they involved in other palmitoylation dependent cellular functions apart from structural re-enforcement?

To reflect the reviewer's point, we have added the following to the Discussion section: "Mutation of the N-terminal cysteine motif of IMC1a (Mutant 1) causes more severe phenotypes than substitution of the C-terminal cysteine motif (Mutant 2) with regards to IMC1a stability (Fig. 3A) and infectivity to the salivary glands (Table 1). This difference could reflect quantitative differences in palmitoylation at the N- and C-terminus, as predicted (Fig. 1). Alternatively, the cysteine motifs may possess additional roles besides acting as palmitoylation sites, which could be different between the N- and C-terminus." (lines 398-403).

In the Graphical abstract the bulging portion of the sporozoite seems to be slightly different between the three parasite lines. Is this representative of all the sporozoites in the mutant population?

The images shown in the graphical abstract are typical, but the position of the bulging area in the mutant sporozoites can be located anywhere between one end and the middle of the sporozoite, as reported previously for IMC1a knockout sporozoites (Khater et al., 2004).

Apart from IMC1 do the other Toxoplasma homologues of the alveolins have the cysteine residues conserved? Would it be worthwhile showing this in figure 1? This (Foe et al., Cell host microbe 2015) may be a valuable reference on the global Palmitome in Toxoplasma.

A subset of *Toxoplasma* alveolins possess similar conserved terminal cysteine motifs (IMC1, IMC4, IMC14 and IMC15) (Anderson-white et al., 2011) and this has now been added to the Introduction (lines 67-69) rather than to Fig. 1. Of these, IMC1, IMC4 and IMC14, but not IMC15 are shown to be palmitoylated in tachyzoites (Foe et al., 2015).

Line 210: The sentence belongs in the methods section.
This sentence has now been moved to section 2.4 of the Materials and Methods (lines 153-154).

Line 236: The fluorescent levels as shown by Fig. 2 are better shown as black and white images and ideally should be quantified.
As requested we are now showing Fig. 2 (and Fig. 4) in black and white. The IMC1a levels were quantified by western blot and the values stated in the text (line 242). This is a much better way than quantifying the fluorescence of individual oocysts, as the values obtained reflect the entire sporozoite population and can be normalized.

Line 275: It would be nice to show representative images of midgut sporozoites in the supplement to validate this statement.

As requested we have added a supplemental Fig. S2 showing representative images of midgut sporozoites of WT, Mutant 1 and Mutant 2.

Line 280-293: How does the sporozoite infectivity reduction observed in mosquitoes relate to transmission to the rodent? Data should be shown if just numbers of infected mice per total mice challenged. Considering that mutants 1,2, all have intermediate phenotypes compared to the knockout it would be sensible to suggest that transmission into mice would also be partially rescued?

To address the reviewer's point we have added the following to the Results section: "The lack of mosquito transmission of Mutant 1 could be caused by the low numbers of salivary gland sporozoites, or by a reduced sporozoite infectivity to the mouse, or a combination of both. Because of the low numbers of salivary gland sporozoites that could be obtained from Mutant 1-infected mosquitoes, sporozoite infectivity to the mouse by needle injection was not assessed." (lines 290-294). Nonetheless, the results (Table 1) clearly show that Mutant 1 and Mutant 2 possess intermediate phenotypes with regards to sporozoite infectivity.

Line 290-293: Was there an attempt to also try and transmit the mutant 1 parasites intravenously?

No, see previous point.

Line 301: What would happen if all the cysteines were deleted i.e both the N and C terminal ones? It's not necessary to do the experiment but please speculate.

A 'double' mutant would likely result in even greater protein instability and reductions in IMC1a levels than the single mutations, and hence a phenotype more similar to the knockout.

Line 316: There is no data to back this claim.

We have removed this sentence.

Line 456 and 458: The references are not consistent with the rest (journal name).

We have corrected the references' format.

Table 1: please report meaningful numbers, 10,938 is not a sensible number, make it 11.000 and adjust similarly all the other figures in the table.

As requested we have now rounded the numbers in the table.

Put scale bars on all figures with images.

Scale bars have now been added to Figs. 2 and 4.
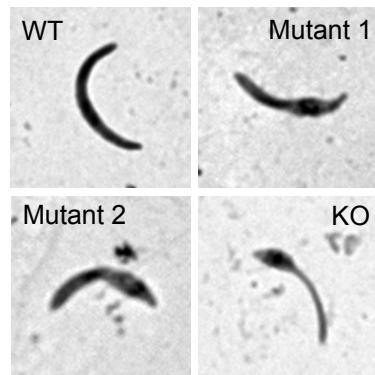
- The terminal cysteine motifs of the alveolin IMC1a stabilise the protein

- IMC1a depletion dose-dependently affects sporozoite morphogenesis

- Sporozoite size correlates with sporozoite infectivity

1   **The *Plasmodium* alveolin IMC1a is stabilised by its terminal cysteine motifs and facilitates sporozoite**

2   **morphogenesis and infectivity in a dose-dependent manner**

3

4

5   *Fatimah S. Al-Khattaf, Annie Z. Tremp, Amira El-Houderi, and Johannes T. Dessens*

6

7

8   Department of Pathogen Molecular Biology, London School of Hygiene & Tropical Medicine, Keppel

9   street, London WC1E 7HT, United Kingdom

10

11

12   To whom correspondence should be addressed: Johannes T. Dessens, London School of Hygiene &

13   Tropical Medicine, Keppel street, London WC1E 7HT, United Kingdom, Telephone: (44) 2079272865;

14   FAX: (44) 2076374314; E-mail: Johannes.Dessens@lshtm.ac.uk

15

16

17   Supplementary data associated with this article

18

19 **Abstract**

20 Apicomplexan parasites possess a unique cortical cytoskeleton structure composed of intermediate

21 filaments. Its building blocks are provided by a conserved family of proteins named alveolins. The core

22 alveolin structure is made up of tandem repeat sequences, thought to be responsible for the filamentous

23 properties of these proteins. A subset of alveolins also possess conserved motifs composed of three closely

24 spaced cysteine residues situated near the ends of the polypeptides. The roles of these cysteine motifs and

25 their contribution to alveolin function remains poorly understood. The sporozoite-expressed IMC1a is

26 unique within the *Plasmodium* alveolin family in having conserved cysteine motifs at both termini. Using

27 transgenic *Plasmodium berghei* parasites, we show in this structure-function analysis that mutagenesis of

28 the amino- or carboxy-terminal cysteine motif causes marked reductions in IMC1a protein levels in the

29 parasite, which are accompanied by partial losses of sporozoite shape and infectivity. Our findings give

30 new insight into alveolin function, identifying a dose-dependent effect of alveolin depletion on sporozoite

31 size and infectivity, and vital roles of the terminal cysteine motifs in maintaining alveolin stability in the

32 parasite.

33

1. Introduction

Plasmodium species, the causative agents of malaria, have a complex life cycle in vertebrate host and mosquito vector. Among the many different developmental forms of the parasite feature three motile and invasive stages (also known as 'zoites'): the ookinete, sporozoite and merozoite. The zoites of *Plasmodium*, as well as those of related apicomplexan parasites, possess an unusual cortical structure termed the pellicle. The pellicle is defined by a double membrane structure termed the inner membrane complex (IMC) situated directly underneath the plasma membrane, which is equivalent to a system of flattened sacs or alveoli [1-3]. On the cytoplasmic face of the IMC is anchored a network of intermediate filaments termed the subpellicular network (SPN), the function of which is to support the pellicle membranes and give the cell mechanical strength [4].

A family of proteins now termed alveolins have been identified as components of the SPN [4, 5]. The alveolin superfamily includes structurally related proteins from apicomplexan parasites, ciliates and dinoflagellate algae, the three phyla comprising the Alveolata superphylum [6]. In the genus *Plasmodium*, 13 conserved and syntenic alveolin family members have been identified that are differentially expressed among the three different zoites stages of malaria parasites [7, 8]. It has been shown in the rodent malaria species *P. berghei* that disruption of alveolins gives rise to morphological aberrations that are accompanied by reduced tensile strength of the zoite stages in which they are found [5, 8-11]. In *Tetrahymena thermophila*, knockdown of the alveolin TtALV2 was also reported to affect cell morphology [12], indicating that alveolin functions, like their structures, are evolutionary conserved. *Plasmodium* alveolins also have roles in parasite gliding motility [5, 9-11] most likely by tethering glideosome associated proteins that reside in the IMC.

The alveolins identified in *Plasmodium* are characterised by having one or more highly conserved domains separated by regions of variable length and amino acid composition. These conserved 'alveolin' domains are composed of tandem repeat sequences [7, 12]. This has revealed an interesting parallel with metazoan intermediate filament proteins such as lamins and keratins, whose underlying architectures include a helical rod domain that can form coiled-coils by virtue of a seven amino acid tandem repeat structure [13]. These coiled-coil domains are thought to be fundamental for the filament-forming properties

62   of these molecules. Apart from the conserved alveolin domains, a subset of the alveolins also possess

63   conserved cysteine motifs close to their amino- or carboxy-terminus (Fig. 1). These motifs are made up of a

64   single cysteine and a double cysteine that are separated by a small number of other amino acids (Fig. 1).

65   With the exception of IMC1i, The N- and C-terminal motifs are inverted, with the single cysteine located

66   nearest the end of the polypeptide (Fig. 1). The function of these cysteine motifs is largely unknown,

67   although they have been suggested to provide sites for post-translational S-palmitoylation [14] (Fig. 1). A

68   subset of alveolins in *Toxoplasma* (IMC1, IMC4, IMC14 and IMC15) possess similar conserved terminal

69   cysteine motifs [14]. Because these conserved cysteine motifs have not been identified in alveolins from

70   dinoflagellates or ciliates, their function could be related to the unique motility and/or cytokinesis

71   associated with the Apicomplexa [6]. IMC1a is the only *Plasmodium* alveolin with conserved cysteine

72   motifs at both ends, and in this study we employ site-directed mutagenesis and allelic replacement in *P.*

73   *berghei* to investigate the contribution of these motifs to the function of the protein and the SPN as a whole.

74   We also describe a new method for accurate size measurements of sporozoite populations, providing a

75   valuable new tool for assessing sporozoite phenotypes.

76

77

78

2. Materials and Methods

2.1 Animal use

All laboratory animal work is subject to regular ethical review by the London School of Hygiene and Tropical Medicine, and has approval from the United Kingdom Home Office. Work was carried out in accordance with the United Kingdom Animals (Scientific Procedures) Act 1986 implementing European Directive 2010/63 for the protection of animals used for experimental purposes. Experiments were conducted in 6-8 weeks old female CD1 mice, specific pathogen free and maintained in filter cages. Animal welfare was assessed daily and animals were humanely killed upon reaching experimental or humane endpoints. Mice were infected with parasites by intraperitoneal injection, or by infected mosquito bite on anaesthetized animals. Parasitemia was monitored regularly by collecting of a small drop of blood from a superficial tail vein. Drugs were administered by intraperitoneal injection or where possible were supplied in drinking water. Parasitized blood was harvested by cardiac bleed under general anaesthesia without recovery.

2.2 Parasite maintenance, transmission, culture and purification

P. berghei ANKA clone 2.34 parasites were maintained as cryopreserved stabilates or by mechanical blood passage and regular mosquito transmission. Mosquito infection and transmission assays were as previously described using Anopheles stephensi [5, 15] and infected insects were maintained at 20°C at approximately 70% relative humidity.

2.3 Construction of gene targeting vectors

To allow mCherry tagging of IMC1a, an approximately 3.5kb fragment corresponding to the entire *imc1a* gene (introns included) plus 5'-UTR was PCR amplified from *P. berghei* gDNA using primers pDNR-imc1a-F (ACGAAGTTATCAGTCGAGGTACCTTTCATGATTCTATCTATTGTTAATTTTAATTG) and pDNR-imc1a-R (ATGAGGGCCCCTAAGCTTTTATCTTGATTACAAAAATAATTACAACATTTG) and introduced into SalI/HindIII-digested pDNR-mCherry [16] by in-fusion to give plasmid pDNR-IMC1a/mCherry (Fig. S1).

5

106   To substitute the N-terminal cysteine motif of IMC1a (Mutant 1) primers IMC1a-Mut1-F

107   (GAAAATAAATAGTAATCTCGAGCATGATGAGTTGGGAGAAGACA) and IMC1a-Mut1-R

108   (ATTACTATTTATTTTCCATGCATCAAACATTTTAATTAAATG) were used to PCR amplify pDNR-

109   IMC1a/mCherry, and the PCR product was circularized by in-fusion to give plasmid pDNR-IMC1a-Mutant

110   1. Introduction of a diagnostic XhoI site changes the double cysteine (CC) in the amino-terminal motif to

111   leucine-glutamate (LE). To substitute the C-terminal cysteine motif of IMC1a (Mutant 2) primers IMC1a-

112   Mut2-F (CTCGAGAATTATTTTTGGAATCAAGATAAAAGCTTAGGGGC) and IMC1a-Mut2-R

113   (CCAAAAATAATTCTCGAGTTTGTCTTCAGAATTATCACTTTTTTTT) were used to PCR amplify

114   pDNR-IMC1a/mCherry, and the PCR product was circularized by in-fusion to give plasmid pDNR-IMC1a-

115   Mutant 2. Introduction of a diagnostic XhoI site changes the double cysteine (CC) in the carboxy-terminal

116   motif to leucine-glutamate (LE). To substitute the double cysteine from the C-terminal cysteine motif of

117   IMC1a   (Mutant   3)   primers   IMC1a-Mut3-F

118   (CTCGAGAATTATTTTTGTAATCAAGATAAAAGCTTAGGGGC) and IMC1a-Mut3-R

119   (ACAAAAATAATTCTCGAGTTTGTCTTCAGAATTATCACTTTTTTTT) were used to PCR amplify

120   pDNR-IMC1a/mCherry, and the PCR product was circularized by in-fusion to give plasmid pDNR-IMC1a-

121   Mutant 3. This mutation introduces a diagnostic XhoI restriction site, changing the double cysteine (CC) in

122   the carboxy-terminal motif to leucine-glutamate (LE). To substitute the single cysteine from the C-terminal

123   cysteine   motif   of   IMC1a   (Mutant   4)   primers   IMC1a-Mut4-F

124   (TTATTTCGCGAATCAAGATAAAAGCTTAGGGGC)   and   IMC1a-Mut4-R

125   (TTGATTCGCGAAATAATTACAACATTTGTCTTCAGAATTATCACT) were used to PCR amplify

126   pDNR-IMC1a/mCherry, and the PCR product was circularized by in-fusion to give plasmid pDNR-IMC1a-

127   Mutant 4. This mutation introduces a diagnostic NruI restriction site, changing the single cysteine (C) in the

128   carboxy-terminal motif to alanine (A) (Fig. S1).

129   Primers hDHFR/ERI-F (ACAAAGAATTCATGGTTGGTTCGCTAAACT) and hDHFR/ERI-R

130   (ACCATGAATTCTTTGTAACATTTAGGTGTGTATTTATATATATAAGC) were used to PCR amplify

131   plasmid pLP-hDHFR [17]. Template plasmid DNA was removed after the PCR by DpnI digestion, and the

132   PCR product was circularized by in-fusion, to give plasmid pLP-hDHFR/EcoRI. In this plasmid the BamHI

6

133   restriction site site at beginning of the hDHFR gene is replaced with an EcoRI recognition sequence. A 1.7

134   kb fragment corresponding to the *hdhfryfcu* gene was PCR amplified from plasmid pL0035 with primers

135   hDHFRyFCU-F   (ATGTTACAAAGAATTCATGGTTGGTTCGCTAAACTG)   and   hDHFRyFCU-R

136   (AAGAAAAACGGGATCCTTAAACACAGTAGTATCTGTCACCAAAG)   and   introduced   into

137   EcoRI/BamHI-digested pLP-hDHFR/EcoRI by in-fusion to give pLP-hDHFRyFCU. A 0.75 kb fragment

138   corresponding to the 3'UTR of the *imc1a* gene was amplified from *P. berghei* gDNA with primers pLP-

139   imc1a-F (ATATGCTAGAGCGGCCAAAATATGGTATTTTAAAACTATTGAATTGG) and pLP-imc1a-

140   R (CACCGCGGTGGCGGCCAGCGACACTTAAGAGATAGCATAAGA) and introduced into NotI-

141   digested pLP-hDHFRyFCU by in-fusion to give plasmid pLP-hDHFRyFCU/IMC1a.

142   Cre-*lox*p recombination of pDNR-IMC1a/mCherry, pDNR-IMC1a-Mutant 1 and pDNR-IMC1a-

143   Mutant 2, pDNR-IMC1a-Mutant 3 and pDNR-IMC1a-Mutant 4 was carried out with pLP-

144   hDHFRyFCU/IMC1a to give the final targeting vectors pLP-IMC1a/mCherry-WT, pLP-IMC1a/mCherry-

145   Mutant 1 to pLP-IMC1a/mCherry-Mutant 4, respectively.

146   Sequence verification across the IMC1a::mCherry-encoding region identified one targeting vector

147   that had obtained an undesired frameshift close to the 5'-end of the *imc1a* coding sequence. This plasmid

148   was used to generate a new IMC1a null mutant parasite (IMC1a/mCherry-KO) by the same targeting

149   strategy as the other parasite lines.

150

151   *2.4 Generation and genomic analysis of genetically modified parasites*

152   Parasite transfection, pyrimethamine selection and dilution cloning were performed as previously described

153   [18]. The *imc1a* gene targeting strategy employed double crossover homologous recombination, ensuring

154   that its modifications were stable and non-reversible (Fig. S1). Prior to performing transfections, plasmid

155   DNA was double-digested with KpnI and SacII to remove the plasmid backbone. Genomic DNA extraction

156   was performed as previously described [15]. After transfection, drug resistant parasites were subjected to

157   limiting dilution cloning. Integration of the selectable marker gene into the imc1a locus was confirmed by

158   diagnostic   PCR   across   the   3'   integration   site   using   primers   P3

159   (ACAAAGAATTCATGGTTGGTTCGCTAAAC) and P4 (TGCACACCCACCTGATTG) (Fig. S1).

160   Integration of the mCherry-tagged IMC1a-encoding sequence into the imc1a locus was confirmed by

161   diagnostic PCR across the 5' integration site with primers P1 (GCACATTAATGCATTTGGG) and P2

162   (AACGGGATCTTCTAGTTACTTGTACAGCTCGTCCATGC) (Fig. S1). The absence of the unmodified

163   imc1a allele in the clonal parasite lines was confirmed by diagnostic PCR with primers P1 and P4 (Fig. S1).

164

165   *2.5 Sporozoite footprint measurements*

166   Sporozoite-infected tissues were dissected from parasite-infected mosquitoes and the sporozoites gently

167   released in a Dounce homogenizer. Sporozoites were spotted onto glass microscope slides, allowed to

168   adhere and then air dried. After methanol fixation, Giemsa-stained images of individual cells were captured

169   by microscopy on Zeiss LSM510 inverted laser scanning confocal microscope. Using Zeiss LSM image

170   browser software the circumference was measured, and the surface area occupied (i.e. the footprint)

171   calculated. Statistical analysis was carried out using two-tailed t-test.

172

173   *2.6 Western blot analysis*

174   Parasite samples were heated directly in SDS-PAGE loading buffer at 70ºC for 10 min. Proteins were

175   fractionated by electrophoresis through NuPage 4-12% Bis-Tris precast gels (Invitrogen) and transferred to

176   PVDF membrane (Invitrogen) according to the manufacturer's instructions. Membranes were blocked for

177   non-specific binding in PBS supplemented with 0.1% Tween 20 and 5% skimmed milk for 1h at room

178   temperature. Rabbit polyclonal antibody against RFP (Abcam) diluted 1 in 5,000 was applied to the

179   membrane for 1h at room temperature. After washing, membranes were incubated with goat anti rabbit IgG

180   conjugated to horse radish peroxidase (HRP) (Abcam) diluted 1 in 5,000 for 1h at room temperature. After

181   further washing, signal was detected by chemiluminescence (ECL western blotting substrate, Pierce)

182   according to manufacturer's instructions. For reprobing, the blot was incubated in 30% hydrogen peroxide

183   solution for 30min at 37 degrees to inactivate residual HRP [19]. The membrane was reblocked and then

184   incubated with monoclonal antibody 3D11 against circumzoite protein (CSP) diluted 1 in 1000 for 1h at

185   room temperature. After washing secondary goat-anti-mouse polyclonal antibody conjugated to HRP

186 (Invitrogen 81-6520) diluted 1 in 5000 was added and incubated for 1h at room temperature prior to

187 washing and chemilluminescence detection.

188

189 *2.7 RT-PCR analysis*

190 Twenty midguts were harvested from parasite-infected mosquitoes at two weeks post-infection, pooled, and

191 total RNA was extracted using a Qiagen RNeasy mini kit according to manufacturer's instructions. First

192 strand cDNA was synthesized with M-MLV reverse transcriptase, (RNase H minus point mutation;

193 Promega) using oligo(dT)25 as primer, for 1h at 50°C. Excess primer was removed by column purification

194 (Qiaquick gel extraction kit; Qiagen) and the eluted cDNA was subjected to PCR amplification with

195 primers A30 (ATATAGTCCATTTAGTTAGAGTTTGTG) and pDNR-imc1a-R

196 (ATGAGGGCCCCTAAGCTTTTATCTTGATTACAAAAATAATTACAACATTTG)

197 to amplify imc1a, and primers tub1-F (GAAGTAATAAGTATACATGTAGG) and tub1-R

198 (ACACATCAATGACTTCTTTACC) to amplify tubulin 1.

199

200 *2.8 Microscopy*

201 For assessment of fluorescence, live parasite samples were assessed, and images captured, on a Zeiss

202 LSM510 inverted confocal microscope and Zeiss LSM image browser software. For comparison of samples,

203 images were captured with the same settings using the 'reuse' function.

204

205

3. Results

3.1 The terminal cysteine motifs of IMC1a affect protein stability

To study expression and localization of IMC1a and variants of it in the parasite, we first generated a transgenic *P. berghei* line that expresses full-length IMC1a fused to a carboxy-terminal mCherry tag (Fig. S1), named IMC1a/mCherry-WT. To study the contribution of the cysteine motifs to IMC1a function, mutations substituting the three cysteines were introduced by site-directed mutagenesis removing either the N-terminal motif (named IMC1a/mCherry-Mutant 1) or the C-terminal motif (named IMC1a/mCherry-Mutant 2) (Fig. S1). The mutations introduced a diagnostic XhoI restriction site in order to screen targeting vectors and transgenic parasites for the presence of the desired mutation. Introduction of this XhoI site changes the double cysteine (CC) to a leucine-glutamate (LE) (Fig. S1). In addition, an IMC1a/mCherry targeting vector that contained a frame shift very near the 5' end of the coding sequence was used to generate a new IMC1a null mutant parasite line (named IMC1a/mCherry-KO) using the same genetic approach as the other IMC1a lines (Fig. S1).

Parasite line IMC1a/mCherry-WT developed normally in mouse and mosquito, and was readily transmitted by sporozoite-infected mosquito bite, demonstrating that the mCherry tag did not interfere with normal IMC1a function. Using fluorescence microscopy, strong mCherry-based fluorescence was detected in sporulating oocysts (Fig. 2A). In both midgut and salivary gland sporozoites, the fluorescence was concentrated at the cell periphery (Fig. 2A) consistent with the location of the SPN. Western blot analysis of sporozoite lysates using anti-mCherry antibodies detected one major band migrating at approximately 130kDa, corresponding to the IMC1a::mCherry fusion protein (Fig. 2B). Some smaller proteins of much lower intensity were also detected probably resulting from low level proteolytic processing/degradation. As expected, IMC1a/mCherry-KO parasites did not exhibit mCherry fluorescence in oocysts or sporozoites (Fig. 2C), because the mCherry tag is not expressed due to an upstream frameshift. IMC1a/mCherry-KO oocysts displayed a phenotype comparable to that previously described for IMC1a null mutants [5], producing numbers of sporozoites similar to its WT counterpart (mean midgut oocysts/sporozoites per mosquito IMC1a/mCherry-WT: 43/15,000; IMC1a/mCherry-KO: 52/17,000; n=10), but with abnormal size and shape (Fig. 2C).

233   Parasite lines IMC1a/mCherry-Mutant 1 and Mutant 2 also displayed mCherry-based fluorescence

234   in mature oocysts and sporozoites (Figs. 2DE), as expected, demonstrating that the full-length IMC1a

235   protein was expressed. However, in both mutants the fluorescence levels were markedly lower compared to

236   parasite line IMC1a/mCherry-WT (Fig. 2A). These observations indicated that the removal of the amino- or

237   carboxy-terminal cysteine motif from IMC1a had adversely affected either the amount of the alveolin in the

238   parasite, or the ability of its mCherry moiety to fluoresce. To distinguish between these possibilities, we

239   quantified the amounts of IMC1a in sporozoite samples of the different parasite lines by western blot

240   analysis. The values obtained revealed that, relative to circumsporozoite protein (CSP), significantly

241   reduced amounts of IMC1a::mCherry fusion protein were present in Mutant 1 and Mutant 2 (on average

242   10% and 21% of WT levels, respectively; $P<0.001$; n=3) (Fig. 3A). These reduced levels of

243   IMC1a::mCherry fusion protein in the parasite explain the lower fluorescence levels observed in Mutant 1

244   and Mutant 2. Sporozoites of IMC1a/mCherry-Mutant 1 had consistently lower levels of IMC1a than

245   Mutant 2, although the differences were not statistically significant (P=0.09).

246   Because all the transgenic parasite lines used in this study were generated with the same gene

247   targeting strategy, and express IMC1a from the same, native *imc1a* promoter (Fig. S1), *imc1a* gene

248   expression at the transcription level should not be affected. To confirm this, we carried out reverse

249   transcription-PCR analysis on sporulating oocysts. This was done with Mutant 1 - which showed the lowest

250   IMC1a protein level - in direct comparison with the control parasite line IMC1a/mCherry-WT, and

251   normalised against the reference tubulin 1 gene (*tub1*). Primers for *imc1a* amplified a mRNA-specific 2.4kb

252   product, and a gDNA-specific 2.8kb product (due to introns), while primers for *tub1* mainly amplified a

253   mRNA-specific 0.35kb product (the product amplified from gDNA is 1.0kb due to introns [7]) (Fig. 3B).

254   Measured band intensities normalised against the reference *tub1* gene showed that IMC1a/mCherry-Mutant

255   1 oocysts contained approximately 1.5-fold more *imc1a* mRNA than its WT counterpart. Accordingly, the

256   reduced levels of IMC1a present in Mutant 1, and by analogy in Mutant 2, are unlikely to be caused by a

257   reduced *imc1a* gene expression at the transcription level.

258

259   *3.2 The terminal cysteine motifs of IMC1a affect sporozoite shape*

260   Microscopic examination of sporozoites from IMC1a/mCherry-Mutant 1 and Mutant 2 indicated that they

261   had an abnormal shape (Fig. 2). Although this shape was reminiscent of the shape of IMC1a null mutant

262   sporozoites, it appeared less severe than is the case after a complete knockout of IMC1a expression (Fig.

263   2C). Because of the variable and irregular shapes of the mutant sporozoites, their size was difficult to define

264   by linear measurements of length and width. Thus, we developed a more sensitive measure of the observed

265   changes in sporozoite morphology by determining their 'footprint', which gives a quantitative measure of

266   the sporozoite's size independent of its shape. Footprint data were collected by measuring the surface area

267   occupied by Giemsa-stained sporozoites dried onto microscope slides, and showed that KO sporozoites

268   were on average significantly smaller than WT sporozoites ($P<0.0001$, $n=27$), in fact less than half the

269   normal size (Fig. 3C). Sporozoites of Mutant 1 and Mutant 2 had intermediate sizes, both being

270   significantly smaller that WT sporozoites ($P<0.0001$, $n=27$), but significantly larger than KO sporozoites

271   ($P<0.0001$, $n=27$) (Fig. 4C). Mutant 1 sporozoites were on average smaller than those of Mutant 2, albeit

272   the differences were not statistically significant ($P=0.07$, $n=27$) (Fig. 3C). These observations demonstrate

273   that mutations of the terminal cysteine motifs of IMC1a cause intermediate phenotypes with regards to

274   sporozoite shape and size, compared to null mutants. We did not observe discernible shape/size differences

275   between midgut- and salivary gland-derived sporozoite populations within our mutant lines (data not shown,

276   and Fig. S2), pointing to similar infectivity levels throughout the population irrespective of sporozoite

277   size/shape.

278

279   *3.3 The terminal cysteine motifs of IMC1a affect sporozoite infectivity*

280   We analyzed the effects of the cysteine mutations on sporozoite infectivity by infecting *Anopheles*

281   *stephensi* vector mosquitoes. The reference parasite line IMC1a/mCherry-WT gave rise to high numbers of

282   salivary gland sporozoites (Table 1) that were readily transmissible by mosquito bite. In sharp contrast, our

283   IMC1a null mutant sporozoites were unable to reach the salivary glands in detectable numbers (Table 1) in

284   full agreement with a previous study [5]. Salivary gland sporozoite numbers for Mutant 2 were consistently

285   lower (3- to 4-fold) than those observed for IMC1a/mCherry-WT parasites (Table 1), pointing to a reduced

286   infectivity to the salivary glands. Nonetheless, Mutant 2 sporozoites could be transmitted to mice by

287   mosquito bite, and after transmission the phenotype of Mutant 2 remained unchanged with respect to

288   fluorescence level, sporozoite size and infectivity (data not shown). In contrast to Mutant 2, salivary gland

289   sporozoite numbers for Mutant 1 were markedly reduced (>10-fold) (Table 1), and we were repeatedly

290   (n=5) unable to transmit this parasite by mosquito bite. The lack of mosquito transmission of Mutant 1

291   could be caused by the low numbers of salivary gland sporozoites, or by a reduced sporozoite infectivity to

292   the mouse, or a combination of both. Because of the low numbers of salivary gland sporozoites that could

293   be obtained from Mutant 1-infected mosquitoes, sporozoite infectivity to the mouse by needle injection was

294   not assessed. Nonetheless, the combined results demonstrate that IMC1a/mCherry-Mutant 1 and Mutant 2

295   possess intermediate phenotypes with regards to sporozoite infectivity. These infectivity data are consistent

296   with and supported by the other phenotypes reported in this paper (IMC1a expression level, sporozoite

297   shape and size).

298

299   *3.4 Properties of the carboxy-terminal cysteine motif are determined by the di-cysteine*

300   In contrast to the N-terminal cysteine motif of IMC1a, where all three cysteine residues are predicted to be

301   palmitoylated (Fig. 1), within the C-terminal cysteine motif the di-cysteine, but not the single cysteine, are

302   predicted to be palmitoylated (Fig. 1). If this prediction is accurate and palmitoylation were indeed key to

303   the role of the terminal cysteine motifs, then substitution of the single cysteine of the C-terminal motif

304   should have little effect on IMC1a stability and function, while substitution of the di-cysteine should

305   resemble the Mutant 2 phenotype. To test this hypothesis, we generated two more mutants of the carboxy-

306   terminal cysteine motif in IMC1a, in which either its di-cysteine (named IMC1a/mCherry-Mutant 3) or its

307   single cysteine (named IMC1a/mCherry-Mutant 4) were substituted (Fig. S1). Subsequent phenotypic

308   assessment revealed that Mutant 4 parasites were indistinguishable from their WT counterparts displaying

309   bright fluorescence that was concentrated at the cortex of normal shaped sporozoites (Fig. 4B). By contrast,

310   Mutant 3 oocysts and sporozoites displayed markedly lower fluorescence levels (Fig. 4A) and were

311   indistinguishable from those of Mutant 2. Footprint measurements confirmed that the average size of

312   Mutant 4 sporozoites was similar to that of IMC1a/mCherry-WT sporozoites (P=0.99, n=27) (Fig. 4C),

313   while Mutant 3 sporozoites were indistinguishable from those of IMC1a/mCherry-Mutant 2 in terms of

314   shape and size (P=0.38, n=27) (Fig. 4C). In terms of infectivity, too, Mutant 4 resembled its WT

315   counterpart, while Mutant 3 behaved like Mutant 2 (Table 1). These data show that the double cysteine

316   (CC) contributes primarily to the properties of the carboxy-terminal cysteine motif, as evidenced by the

317   same wildtype phenotypes of the IMC1a/mCherry-WT (CC...C) and Mutant 4 (CC...A) parasite lines, as

318   well as the same intermediate phenotypes of the IMC1a/mCherry-Mutant 3 (LE...C) and Mutant 2 (LE...W)

319   parasite lines. These data are consistent with the hypothesis that the di-cysteine is most likely a

320   palmitoylation site, as predicted (Fig. 1). Moreover, the single cysteine within the same motif is not

321   required for this lipid modification to occur.

322

323

4. Discussion

In this study we have employed red fluorescent protein tagging in transgenic *P. berghei* parasites to study the function of the terminal cysteine residues of the alveolin IMC1a. The results obtained confirm the subcellular localisation and expression of IMC1a in the SPN of sporozoites, and show that mutagenesis of its conserved terminal cysteine motifs results in decreased protein stability causing markedly reduced levels of IMC1a protein, but not *imc1a* transcript, in the parasite. This, in turn, affects sporozoite shape, size and infectivity. We did not observe sporozoites with high (WT) levels of fluorescence in our mutant sporozoite populations. Assuming that IMC1a expression was not affected by the cysteine mutations, this suggests that the reductions in IMC1a levels occurred soon after translation and possibly before IMC1a recruitment to the pellicle.

One possible explanation for the alveolin instability is that the removal of cysteines in the mutant proteins has changed their ability to form specific sulphur bridges, leading to a degree of misfolding and degradation. Arguing strongly against this concept, however, is the localisation of IMC1a in the cytoplasm, a reducing environment that disfavours formation of intra- or intermolecular sulphur bridges [20]. A more likely explanation for the observed alveolin instability is that the removal of cysteine residues in IMC1a adversely affected the ability of this protein to be palmitoylated. S-palmitoylation is a post-translational thioester linkage of the 16-carbon fatty acid palmitate to cysteine residues that plays key roles in protein traffic, localisation, interaction and stability [21]. The conserved terminal cysteine motifs of the *Plasmodium* alveolins are predicted with high confidence to constitute palmitoylation sites (Fig. 1). Combined data from various *Plasmodium* proteomics studies reveal that at least six alveolins are detected in blood stage parasites [22-29]. Among these six only two, IMC1c and IMC1g, possess conserved terminal cysteine motifs (at the carboxy- and amino-terminus, respectively) (Fig. 1). Only IMC1c and IMC1g were detected in the *P. falciparum* blood stage palmitome [30], providing compelling experimental support for a link between these motifs and palmitoylation. Palmitoylation is known to affect protein stability [21], and indeed other known palmitoylated proteins associated with the parasite pellicle (e.g. *Pf*GAP45 and *Pf*MTIP) have been reported to become unstable and degraded when palmitoylation was interfered with using palmitoylation inhibitors or mutagenesis of palmitoylation sites [30]. Unfortunately, the relatively

15

351 small numbers of sporozoites that can be obtained from mosquitoes - a major impediment to biochemical

352 analysis [31] - combined with the presence of a second palmitoylation site at the other end of the protein,

353 and the highly reduced levels of IMC1a in Mutants 1 and 2, made it impossible to demonstrate that the

354 terminal cysteine motifs of IMC1a are palmitoylation sites as predicted. Nonetheless, a molecular role for

355 the terminal cysteine residues of IMC1a as substrates for palmitoylaton seems likely, and indeed is

356 supported by our observation that mutagenesis of the C-terminal single cysteine residue, not predicted to be

357 palmitoylated (Fig. 1), has no discernible effect on IMC1a stability and function (Fig. 4). Palmitoylation of

358 alveolins is thought to promote their association with the IMC via lipid anchoring into the inner membrane

359 [14]. Reductions in IMC1a palmitoylation caused by the cysteine mutations could adversely affect this

360 process and/or protein folding or interaction, which in turn could result in instability and degradation [32].

361 Gene disruption studies of different *P. berghei* alveolins have revealed very similar loss-of-function

362 phenotypes adversely affecting morphology, motility and tensile strength [5, 8-11], indicating that alveolins

363 contribute to the function of the SPN through a similar mechanism. While co-expressed alveolins make

364 distinct contributions to SPN function in a given zoite, these differences appear to be mainly quantitative.

365 For example, null mutants sporozoites of the alveolin IMC1h have an abnormal shape and reduced

366 infectivity not dissimilar from IMC1a null mutants [10]. However, in contrast to the latter, IMC1h-KO

367 sporozoites retain infectivity to the insect's salivary glands [11]. Re-examination of the IMC1h-KO

368 sporozoite size with the footprint method developed here shows that they are indeed significantly smaller

369 (P<0.001) than their wildtype counterparts (parasite line IMC1h/GFP), but also significantly larger

370 (P<0.0001) than IMC1a null mutant sporozoites (footprint IMC1h/GFP: 10.51 ± 0.41 μm^2; IMC1h-KO:

371 7.98 ± 0.44 μm^2). These observations reveal a correlation between sporozoite size and infectivity, which is

372 corroborated by the results of the current IMC1a study.

373 The intermediate phenotypes of IMC1a/mCherry-Mutant 1 and Mutant 2 with regards to sporozoite

374 shape, size and infectivity (Figs. 2, 3, Table 1) indicate that the heavily depleted amount of IMC1a protein

375 in their sporozoites remains at least partly functional, possibly because of a degree of functional redundancy

376 between the amino- and carboxy-terminal cysteine motifs. The low levels of IMC1a::mCherry in these

377 mutants did not allow a definitive allocation of the fusion protein in the sporozoite SPN by fluorescence

378 microscopy (Fig. 2). However, complete failure to localise to the functional site would be expected to result

379 in a null mutant phenotype, which is clearly not the case. In further support for this notion, subcellular

380 localisation of PfGAP45 lacking its palmitoylation site was shown to be unaffected, remaining at the IMC

381 of developing merozoites [30]. Our Mutant 1 and Mutant 2 parasite lines are in effect IMC1a knockdowns,

382 and combined with our observations that the severity of the phenotypes correlates well with the levels of

383 IMC1a found in the parasite, this strongly indicates that IMC1a facilitates sporozoite morphogenesis and

384 infectivity in a dose-dependent fashion. This demonstrates for the first time a link between the amount of

385 alveolin in the zoite and its infectivity. Accordingly, SPN function in the cell would be governed not only

386 by the repertoire of co-expressed alveolins, but also by the level of their expression. Fitting with the nature

387 of structural proteins, this finding suggests that the relative abundance of an alveolin in the cell may

388 determine its relative contribution to the cortical cytoskeleton. In support of this concept, it is perhaps not a

389 coincidence that knockout of the ookinete-expressed alveolin IMC1d has no detectable phenotype, and also

390 has the lowest expression level of all ookinete-expressed alveolins examined by us [7, 9, 10, 16]. Just a

391 fraction of IMC1a (10%-21% of WT level in Mutant 1 and Mutant 2) is sufficient to partially restore the

392 phenotype of IMC1a null mutant parasites (Fig. 4C, Table 1), which points to a non-linear correlation

393 between alveolin level and phenotype, possibly due to the complexity of interactions with other alveolins

394 and SPN components. The loss of infectivity of IMC1a null mutants is attributable to not just the reduced

395 size and abnormal shape of the sporozoites, but also to accompanying reductions in motility (approximately

396 5-fold) and tensile strength of the sporozoites [5]. By inference, the markedly reduced levels of IMC1a

397 present in sporozoites of Mutant 1 and Mutant 2 (Fig. 3A) would result in reduced levels of motility and

398 tensile strength, contributing to the observed losses in sporozoite infectivity in these parasite lines. Mutation

399 of the N-terminal cysteine motif of IMC1a (Mutant 1) causes more severe phenotypes than substitution of

400 the C-terminal cysteine motif (Mutant 2) with regards to IMC1a stability (Fig 3A) and infectivity to the

401 salivary glands (Table 1). This difference could reflect quantitative differences in palmitoylation at the N-

402 and C-terminus, as predicted (Fig. 1). Alternatively, the cysteine motifs may possess additional roles

403 besides acting as palmitoylation sites, which could be different between the N- and C-terminus.

404   TgIMC1, the *T. gondii* orthologue of *Plasmodium* IMC1a, contains similar N- and C-terminal

405   terminal cysteine motifs [4, 5]. However, the C-terminal cysteine motif of TgIMC1 has several additional

406   downstream cysteine residues and is not predicted to be palmitoylated with the method used here. Studies

407   on TgIMC1 revealed a specific proteolytic cleavage near the carboxy-terminus of the protein upstream of

408   its cysteine motif [33]. This cleavage coincides with the maturation of young parasites with a detergent-

409   labile SPN into mature parasites with a detergent-resistant SPN. Ablation of this cleavage through

410   mutagenesis of certain cysteines prevented the SPN to mature and become detergent-resistant [33]. In the

411   case of *P. berghei* IMC1a, there is little evidence for a similar cleavage event. Western analysis of our

412   parasite lines expressing IMC1a fused to a carboxy-terminal mCherry tag shows that sporozoites contain

413   predominantly full-length IMC1a::mcherry fusion product (Fig. 2B), and that if such a cleavage occurred in

414   *Plasmodium* it would at best affect a very small proportion of the protein. It cannot be ruled out that the

415   mCherry tag stopped the protease responsible from reaching the C-terminal cleavage site, preventing the

416   IMC1a cleavage in our parasite lines. Arguing against this possibility, however, is the fact that mCherry

417   tagging of IMC1a did not affect its subcellular localisation or cause a detectable phenotype, which indicates

418   that IMC1a function was not affected. The apparent absence of this cleavage in IMC1a is more likely to

419   reflect specific differences between *Toxoplasma* and *Plasmodium*. The formation of *Plasmodium*

420   sporozoites within a protective oocyst capsule may have eliminated the need to develop within the

421   protection of mechanically stable and rigid mother cell as is the case in *Toxoplasma*.

422

423

424

437   **References**

438

439   [1] Bannister LH, Hopkins JM, Fowler RE, Krishna S, Mitchell GH. A brief illustrated guide to the

440   ultrastructure of *Plasmodium falciparum* asexual blood stages. Parasitol Today. 2000;16:427-33.

441   [2] Morrissette NS, Sibley LD. Cytoskeleton of apicomplexan parasites. Microbiol Mol Biol Rev.

442   2002;66:21-38.

443   [3] Santos JM, Lebrun M, Daher W, Soldati D, Dubremetz JF. Apicomplexan cytoskeleton and motors: key

444   regulators in morphogenesis, cell division, transport and motility. Int J Parasitol. 2009;39:153-62.

445   [4] Mann T, Beckers C. Characterization of the subpellicular network, a filamentous membrane skeletal

446   component in the parasite *Toxoplasma gondii*. Mol Biochem Parasitol. 2001;115:257-68.

447   [5] Khater EI, Sinden RE, Dessens JT. A malaria membrane skeletal protein is essential for normal

448   morphogenesis, motility, and infectivity of sporozoites. J Cell Biol. 2004;167:425-32.

449   [6] Gould SB, Tham WH, Cowman AF, McFadden GI, Waller RF. Alveolins, a new family of cortical

450   proteins that define the protist infrakingdom Alveolata. Mol Biol Evol. 2008;25:1219-30.

451   [7] Al-Khattaf FS, Tremp AZ, Dessens JT. *Plasmodium* alveolins possess distinct but structurally and

452   functionally related multi-repeat domains. Parasitol Res. 2015;115:631-39.

453   [8] Kaneko I, Iwanaga S, Kato T, Kobayashi I, Yuda M. Genome-wide identification of the target genes of

454   AP2-O, a *Plasmodium* AP2-family transcription factor. PLoS Pathog. 2015;11:e1004905.

455   [9] Tremp AZ, Khater EI, Dessens JT. IMC1b is a putative membrane skeleton protein involved in cell

456   shape, mechanical strength, motility, and infectivity of malaria ookinetes. J Biol Chem. 2008;283:27604-11.

457   [10] Tremp AZ, Dessens JT. Malaria IMC1 membrane skeleton proteins operate autonomously and

458   participate in motility independently of cell shape. J Biol Chem. 2011;286:5383-91.

459   [11] Volkmann K, Pfander C, Burstroem C, Ahras M, Goulding D, Rayner JC, et al. The alveolin IMC1h is

460   required for normal ookinete and sporozoite motility behaviour and host colonisation in *Plasmodium*

461   *berghei*. PLoS One. 2012;7:e41409.

462   [12] El-Haddad H, Przyborski JM, Kraft LG, McFadden GI, Waller RF, Gould SB. Characterization of

463   TtALV2, an essential charged repeat motif protein of the *Tetrahymena thermophila* membrane skeleton.

464   Euk Cell. 2013;12:932-40.

465   [13] Herrmann H, Aebi U. Intermediate filaments: molecular structure, assembly mechanism, and

466   integration into functionally distinct intracellular scaffolds. Annu Rev Biochem. 2004;73:749-89.

467   [14] Anderson-White BR, Ivey FD, Cheng K, Szatanek T, Lorestani A, Beckers CJ, et al. A family of

468   intermediate filament-like proteins is sequentially assembled into the cytoskeleton of *Toxoplasma gondii*.

469   Cell Microbiol. 2011;13:18-31.

470   [15] Dessens JT, Beetsma AL, Dimopoulos G, Wengelnik K, Crisanti A, Kafatos FC, et al. CTRP is

471   essential for mosquito infection by malaria ookinetes. EMBO J. 1999;18:6221-7.

472 [16] Tremp AZ, Al-Khattaf FS, Dessens JT. Distinct temporal recruitment of *Plasmodium* alveolins to the

473 subpellicular network. Parasitol Res. 2014;113:4177-88.

474 [17] Saeed S, Carter V, Tremp AZ, Dessens JT. *Plasmodium berghei* crystalloids contain multiple LCCL

475 proteins. Mol Biochem Parasitol. 2010;170:49-53.

476 [18] Waters AP, Thomas AW, van Dijk MR, Janse CJ. Transfection of malaria parasites. Methods.

477 1997;13:134-47.

478 [19] Sennepin AD, Charpentier S, Normand T, Sarre C, Legrand A, Mollet LM. Multiple reprobing of

479 Western blots after inactivation of peroxidase activity by its substrate, hydrogen peroxide. Analyt Biochem.

480 2009;393:129-31.

481 [20] Herrmann JM, Riemer J. Three approaches to one problem: protein folding in the periplasm, the

482 endoplasmic reticulum, and the intermembrane space. Antioxid Redox Signal. 2014;21:438-56.

483 [21] Linder ME, Deschenes RJ. Palmitoylation: policing protein stability and traffic. Nat Rev Mol Cell Biol.

484 2007;8:74-84.

485 [22] Hall N, Karras M, Raine JD, Carlton JM, Kooij TW, Berriman M, et al. A comprehensive survey of

486 the *Plasmodium* life cycle by genomic, transcriptomic, and proteomic analyses. Science. 2005;307:82-6.

487 [23] Lasonder E, Ishihama Y, Andersen JS, Vermunt AM, Pain A, Sauerwein RW, et al. Analysis of the

488 *Plasmodium falciparum* proteome by high-accuracy mass spectrometry. Nature. 2002;419:537-42.

489 [24] Florens L, Washburn MP, Raine JD, Anthony RM, Grainger M, Haynes JD, et al. A proteomic view of

490 the *Plasmodium falciparum* life cycle. Nature. 2002;419:520-6.

491 [25] Treeck M, Sanders JL, Elias JE, Boothroyd JC. The phosphoproteomes of *Plasmodium falciparum* and

492 *Toxoplasma gondii* reveal unusual adaptations within and beyond the parasites' boundaries. Cell Host

493 Microbe. 2011;10:410-9.

494 [26] Bowyer PW, Simon GM, Cravatt BF, Bogyo M. Global profiling of proteolysis during rupture of

495 *Plasmodium falciparum* from the host erythrocyte. Mol Cell Proteomics. 2011;10:M110 001636.

496 [27] Pease BN, Huttlin EL, Jedrychowski MP, Talevich E, Harmon J, Dillman T, et al. Global analysis of

497 protein expression and phosphorylation of three stages of *Plasmodium falciparum* intraerythrocytic

498 development. J Proteome Res. 2013;12:4028-45.

499 [28] Solyakov L, Halbert J, Alam MM, Semblat JP, Dorin-Semblat D, Reininger L, et al. Global kinomic

500 and phospho-proteomic analyses of the human malaria parasite *Plasmodium falciparum*. Nat Comm.

501 2011;2:565.

502 [29] Silvestrini F, Lasonder E, Olivieri A, Camarda G, van Schaijk B, Sanchez M, et al. Protein export

503 marks the early phase of gametocytogenesis of the human malaria parasite *Plasmodium falciparum*. Mol

504 Cell Proteomics. 2010;9:1437-48.

505 [30] Jones ML, Collins MO, Goulding D, Choudhary JS, Rayner JC. Analysis of protein palmitoylation

506 reveals a pervasive role in *Plasmodium development* and pathogenesis. Cell Host Microbe. 2012;12:246-58.

507 [31] Kappe SH, Kaiser K, Matuschewski K. The *Plasmodium* sporozoite journey: a rite of passage. Trends

508 Parasitol. 2003;19:135-43.

509 [32] Resh MD. Covalent lipid modifications of proteins. Curr Biol. 2013;23:R431-5.

510 [33] Mann T, Gaskins E, Beckers C. Proteolytic processing of TgIMC1 during maturation of the membrane

511 skeleton of *Toxoplasma gondii*. J Biol Chem. 2002;277:41240-6.

512

513

514

Figure legends

516

517   **Fig. 1** The *Plasmodium* alveolin cysteine motifs. **A**: Conserved cysteine motifs at the amino- and carboxy-

518   terminal ends of *Plasmodium berghei* alveolins IMC1a (PbANKA_0402600), IMC1c (PbANKA_1202000),

519   IMC1g (PbANKA_1240600), IMC1i (PbANKA_0707100) and IMC1j (PbANKA_1120400). The number

520   of non-cysteine residues (X) adjacent to the conserved terminal cysteines (C) are indicated. Cysteines in red

521   are predicted to be palmitoylated. **B**: Prediction scores of palmitoylated cysteine residues (red) using CSS-

522   Palm 4.0 software (http://csspalm.biocuckoo.org/) and high threshold settings (95% specificity, 90%

523   accuracy).

524

525   **Fig. 2** Phenotypic analyses of mCherry-tagged *Pb*IMC1a parasite lines. **A**: Confocal fluorescence and

526   brightfield images of a sporulating oocyst and sporozoite of parasite line IMC1a/mCherry-WT. **B**: Western

527   blot of a sporozoite lysate of parasite line IMC1a/mCherry-WT (approximately 100,000 sporozoites loaded)

528   using anti-mCherry antibodies, visualising the IMC1a::mCherry fusion protein. Size markers are shown on

529   the left hand side. **C-E**: Confocal images of a sporulating oocyst and sporozoite of mutant parasite lines

530   IMC1a/mCherry-KO (**C**); IMC1a/mCherry-Mutant 1 (**D**); IMC1a/mCherry-Mutant 2 (**E**). Confocal images

531   were captured using the same confocal microscope settings. Scale bars represent 10μm.

532

533   **Fig. 3** Cysteine mutations of IMC1a affect protein stability and sporozoite size. **A**: Western blot of

534   sporozoite lysates from parasite lines IMC1a/mCherry-WT, Mutant 1 and Mutant 2, using anti-mCherry

535   antibodies (*top*), or anti-CSP antibodies (*bottom*). **B**: Reverse transcription PCR analysis of *imc1a* mRNA

536   levels (relative to *tub1* mRNA) in sporulating oocysts of parasite lines IMC1a/mCherry-WT and Mutant 1.

537   **C**: Representative Giemsa-stained sporozoite images from parasite lines IMC1a/mCherry-WT, KO, and

538   Mutants 1-2. Numbers give mean±sem footprint measurements in μm^2 and numbers in brackets give

539   footprint range in μm^2 (n=27).

540

541   **Fig. 4** The double cysteine contributes chiefly to the function of the cysteine motif. Confocal fluorescence

542   and brightfield images of a sporulating oocyst and sporozoite of IMC1a/mCherry-Mutant 3 (**A**) and Mutant

543   4 (**B**). Scale bars represent 10μm. **C**: Representative Giemsa-stained sporozoite images of Mutants 3 and 4.

544   Numbers give mean±sem footprint measurements in μm^2 and numbers in brackets give footprint range in

545   μm^2 (n=27).

546

Table 1 Effects of IMC1a mutations on *Plasmodium berghei* parasite development in *Anopheles stephensi* mosquitoes

Exp.	Parasite line IMC1a/mCherry-	Mean ± sem oocyst number per infected mosquito (n)[a]	Mean salivary gland sporozoite number per infected mosquito[b]
1	WT	39 ± 7 (20)	10,900
	KO	47 ± 8 (20)	0
2	WT	104 ± 42 (10)	6,600
	Mutant 1	97 ± 32 (10)	110
	Mutant 2	98 ± 27 (10)	2,800
3	Mutant 1	94 ± 13 (20)	260
	Mutant 2	133 ± 24 (20)	3,100
4	WT	109 ± 31 (10)	4,900
	Mutant 1	141 ± 50 (10)	220
	Mutant 4	120 ± 44 (10)	5,600
5	Mutant 2	34 ± 9 (20)	2,000
	Mutant 3	36 ± 9 (20)	2,800
6	WT	160 ± 33 (10)	16,600
	Mutant 2	192 ± 30 (10)	3,900
7	Mutant 1	47 ± 11 (10)	330
	Mutant 4	78 ± 25 (10)	9,900

547   [a] n = Number of insects analysed.

548   [b] The same insects were analysed for both oocyst and sporozoite numbers. Oocyst and sporozoite

549   numbers are therefore directly linked, eliminating much of the variability associated with sample size.

550   Oocyst counts were done on individual midguts, sporozoite counts were done on pooled salivary glands
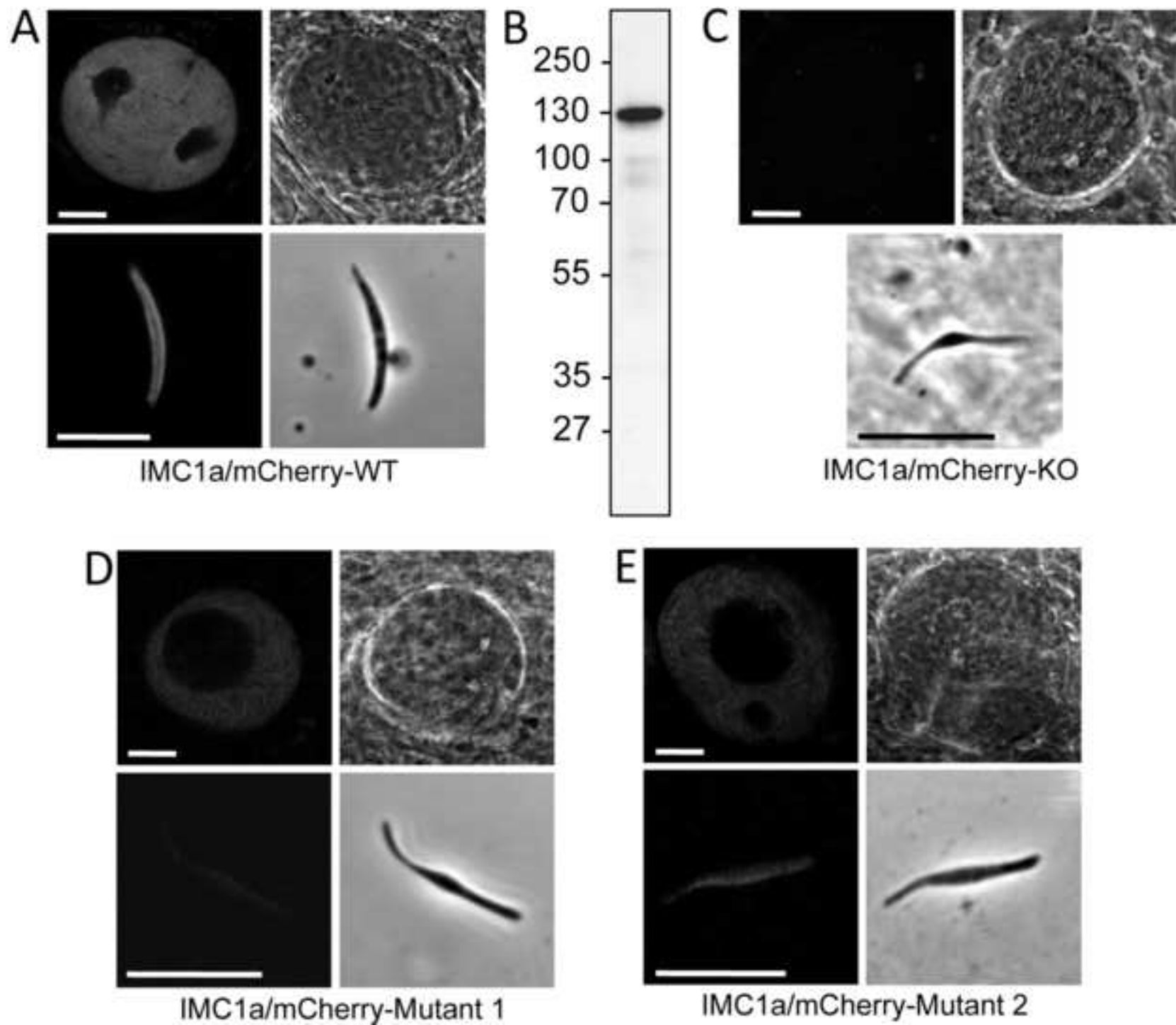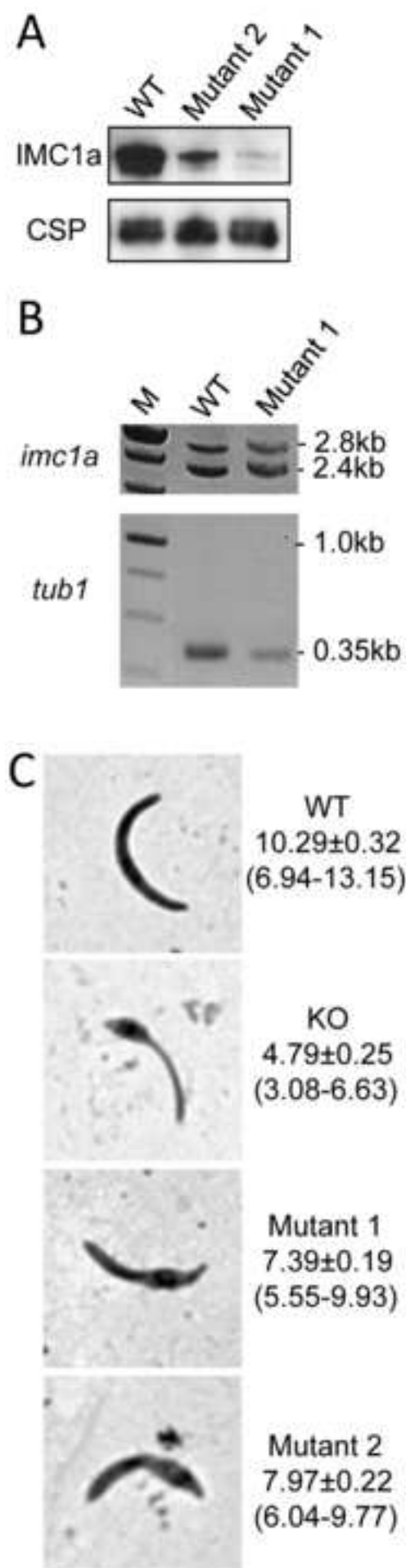
551   from n insects.

552

553

554

Figure 1
Click here to download high resolution image

A

```
IMC1a amino-terminus (4X)C(5X)CC.........CC(3X)C(4X) carboxy-terminus
IMC1c amino-terminus ...................CC(3X)C(1X) carboxy-terminus
IMC1g amino-terminus (1X)C(7X)CC.................. carboxy-terminus
IMC1i amino terminus ...............C(5X)CC(3X) carcoxy-terminus
IMC1j amino-terminus (5X)C(6X)CC.................. carboxy-terminus
```

B

alveolin	Position	Peptide	Score	Cutoff
IMC1a	5	***MFDACKINSNCC	39.45	4.222
IMC1a	11	ACKINSNCCHDELGE	13.588	3.419
IMC1a	12	CKINSNCCHDELGED	36.543	4.222
IMC1a	775	SDNSEDKCCNYFCNQ	15.285	3.419
IMC1a	776	DNSEDKCCNYFCNQD	8.229	4.222
IMC1c	272	EEAKPVGCCTGTCR*	9.35	3.419
IMC1c	273	EAKPVGCCTGTCR**	5.043	4.222
IMC1g	2	******MCSTPNKLA	40.756	4.222
IMC1g	10	STPNKLACCSGDNVF	6.81	3.419
IMC1g	11	TPNKLACCSGDNVFD	38.998	4.222
IMC1i	490	FCNIMNKCCGGE***	14.765	3.419
IMC1j	6	**MENKQCKLIFSDC	34.614	4.222
IMC1j	13	CKLIFSDCCKGRENV	10.098	3.419
IMC1j	14	KLIFSDCCKGRENVA	29.829	4.222

Figure 2

A — IMC1a/mCherry-WT

B — 250, 130, 100, 70, 55, 35, 27

C — IMC1a/mCherry-KO

D — IMC1a/mCherry-Mutant 1

E — IMC1a/mCherry-Mutant 2

A

	WT	Mutant 2	Mutant 1
IMC1a			
CSP			

B

	M	WT	Mutant 1
imc1a			-2.8kb / -2.4kb
tub1			-1.0kb / -0.35kb

C

WT
10.29±0.32
(6.94-13.15)

KO
4.79±0.25
(3.08-6.63)

Mutant 1
7.39±0.19
(5.55-9.93)

Mutant 2
7.97±0.22
(6.04-9.77)

Figure 4

A

IMC1a/mCherry-Mutant 3

B

IMC1a/mCherry-Mutant 4

C

Mutant 3
7.65±0.38
(5.84-9.43)

Mutant 4
10.29±0.27
(7.87-13.36)

Supplementary Material
Click here to download Supplementary Material: Supporting information.pdf